Fate and biological impact of persistent luminescence nanoparticles after injection in mice: a one-year follow-up

Thomas Lécuyer, Johanne Seguin, Alice Balfourier, Marine Delagrange, Pierre Bürckel, René Lai-Kuen, Virginie Mignon, Bertrand Ducos, Michael Tharaud, Bruno Saubaméa, et al.

Fate and biological impact of persistent luminescence nanoparticles after injection in mice: a one-year follow-up †

Thomas Lecuyer,(0000-0002-2283-5450)[a,b], Johanne Seguin,(0000-0001-5689-7046)[a], Alice Balfourier[b], Marine Delagrange[c,d], Pierre Burckel[e], René Lai-Kuen[f], Virginie Mignon[f], Bertrand Ducos,(0000-0002-5322-1339)[c,d], Michael Tharaud,(0000-0001-6131-655X)(Z-5937-2019)[e], Bruno Saubaméa[f], Daniel Scherman[a], Nathalie Mignet,(0000-0002-3323-2997)[a], Florence Gazeau,(0000-0002-6482-3597)[b,‡,*] and Cyrille Richard ,(0000-0003-4896-6675)[a,‡,*]

[a]Université Paris Cité, CNRS, INSERM, UTCBS, Unité de Technologies Chimiques et Biologiques pour la Santé, Faculté de Pharmacie, 75006 Paris, France

[b]Université Paris Cité, CNRS UMR 7057, Matières et Systèmes Complexes (MSC), 75006 Paris, France

[c]High Throughput qPCR Core Facility of the ENS, Université PSL, Institut de Biologie de l'École normale supérieure, F-75005 Paris, France

[d]Laboratoire de Physique de l'École normale supérieure, ENS, Université PSL, CNRS, Sorbonne Université, Université de Paris, F-75005 Paris, France

[e]Université de Paris, Institut de physique du globe de Paris, CNRS, F-75005 Paris, France

[f]Université de Paris, Inserm, CNRS, US25 Inserm, UMS3612 CNRS, Cellular and Molecular Imaging facility, Faculté de Pharmacie de Paris, F-75006, Paris, France

‡These authors contributed equally.

Funding Information

We have combined the funding information you gave us on submission with the information in your acknowledgements. This will help ensure the funding information is as complete as possible and matches funders listed in the Crossref Funder Registry.

Please check that the funder names and award numbers are correct. For more information on acknowledging funders, visit our website: http://www.rsc.org/journals-books-databases/journal-authors-reviewers/author-responsibilities/#funding.

Funder Name :	Agence Nationale de la Recherche
Funder's main country of origin :	
Funder ID :	10.13039/501100001665
Award/grant Number :	ANR-14-CE08-0016-01

Funder Name :	Horizon 2020 Framework Programme
Funder's main country of origin :	
Funder ID :	10.13039/100010661
Award/grant Number :	801305

Funder Name :	Institut de Physique du Globe de Paris

Funder's main country of origin :
Funder ID : 10.13039/501100010768
Award/grant Number : Unassigned

Table of Contents Entry

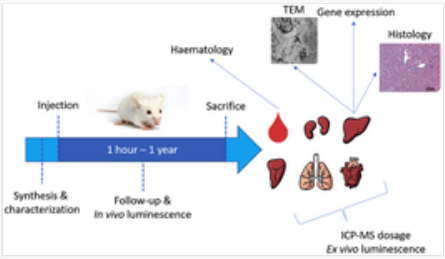

Persistent luminescence nanoparticles (PLNPs) are attracting growing interest for non-invasive optical imaging of tissues with a high signal to noise ratio.

Abstract

Persistent luminescence nanoparticles (PLNPs) are attracting growing interest for non-invasive optical imaging of tissues with a high signal to noise ratio. PLNPs can emit a persistent luminescence signal through the tissue transparency window for several minutes, after UV light excitation before systemic administration or directly *in vivo* through visible irradiation, allowing us to get rid of the autofluorescence signal of tissues. PLNPs constitute a promising alternative to the commercially available optical near infrared probes thanks to their versatile functionalization capabilities for improvement of the circulation time in the blood stream. Nevertheless, while biodistribution for a short time is well known, the long-term fate and toxicity of the PLNP's inorganic core after injection have not been dealt with in depth. Here we extend the current knowledge on $ZnGa_{1.995}O_4Cr_{0.005}$ NPs (or ZGO) with a one-year follow-up of their fate after a single systemic administration in mice. We investigated the organ tissue uptake of ZGO with two different coatings and determined their intracellular processing up to one year after injection. The biopersistence of ZGO was assessed, with a long-term retention, quantified by ICP-MS, mostly in the liver and spleen, parallel with a loss of their luminescence properties. The analysis of the toxicity related to combining an animal's weight, key hematological and metabolic markers, histological observations of liver tissues and quantification of the expression of 31 genes linked to different metabolic reactions did not reveal any signs of noxiousness, from the macro scale to the molecular level. Therefore, the ZGO imaging probe has been proven to be a safe and relevant candidate for preclinical studies, allowing its long term use without any *in vivo* disturbance of the general metabolism.

Introduction

Inorganic nanoparticles (NPs) have emerged as a powerful alternative to organic probes to improve the diagnosis of diseases and their treatment and to assess the efficacy of therapies and the well-being of patients by avoiding side effects.[1,2] The use of NPs for biomedical applications continues to be a rapidly growing research field, with heavy emphasis on imaging and drug delivery.[3] In contrast to molecular based therapeutics,[4–6] NPs possess “scaffolds” to build upon, high surface to volume ratios, shape, and unique properties. While lipid and polymeric NPs have shown useful advantages for drug delivery, such as anti-cancer agents or nucleic acids, inorganic NPs also present advantages and have led to a variety of clinically relevant applications. Among the imaging probes, one of their key assets is the use of light to activate nanoparticles, which presents opportunities for non-invasive diagnosis and therapy for a variety of diseases.[7] For this purpose, our laboratory pioneered the conception and use of persistent luminescence nanoparticles (PLNPs) that have attracted growing interest over the years. Persistent luminescence refers to the phenomenon whereby luminescence lasts for several seconds to a few days after the end of excitation. Hence, the long-lasting phosphorescent nature of PLNPs allows for an experimental design where a complete avoidance of the autofluorescence of the tissues is possible.[8] The past ten years have witnessed several advances to establish near-infrared (NIR) emitting PLNPs as highly sensitive technology for real-time optical imaging in small animals.[9–11] The first generation of PLNPs were based on a silicate matrix doped with rare earth elements (europium and dysprosium) and manganese.[12] Various

materials have been developed with their own specificity such as *in vitro* assays,[13,14] photostimulation[15] or bimodal imaging.[16]

Our laboratory developed $ZnGa_{1.995}O_4Cr_{0.005}$ nanoparticles or ZGO.[17] This doped spinel structure possesses a bright near-infrared (emission = 700 nm) persistent luminescence and can be activated *ex vivo* before injection with UV light, or directly *in vivo* after injection with visible irradiation (excitation = 580 nm). Therefore, after intravenous injection and activation, the ZGO can emit a persistent luminescence signal through the tissue transparency window for several minutes, and thus enable imaging with a high signal to noise ratio, and constitutes a promising alternative to the commercially available optical near infrared probes. More than these unique optical properties, ZGO has shown tunability of size and shape,[18] and versatile functionalization capabilities for both active targeting and improvement of the circulation time in the blood stream.[19,20]

The unique properties of ZGO provide strategic advantages over pure molecular probes, but new complexities must be explored to make NP based applications a viable option in the clinic.[21] Indeed, a key question to assess is the long-term fate of the ZGO after systemic injection. Because of the size of the nanoparticles (>10 nm), renal clearance is impossible[22] and ZGO is cleared from the bloodstream by the mononuclear phagocyte system (MPS).[23] Therefore investigation of the organs and cellular uptake and also determination of their intracellular processing that might result in complete or partial degradation, or storage of bio-persistent NPs in an unchanged form in cells have to be performed.[24,25] In both cases, either the degradation products of ZGO or their accumulation in the tissues as intact NPs could involve toxicity, which could be a limitation for preclinical or clinical use. Indeed, we recently reported that ZGO is degraded *in vitro* in Artificial Lysosomal Fluid (ALF),[26] mimicking the intracellular environment in terms of pH and ionic strength. We and others have also taken interest in the fate and toxicity of PLNPs, mainly focused on *in vitro* assays or based on preliminary and incomplete short- to mid-term *in vivo* evaluations.[27,28]

Therefore, to gain a deeper understanding and to further investigate the biological mechanisms underlying this process, mice were injected with PEGylated ZGO (ZGOPEG) and nonfunctionalized ZGO (ZGOOH) and were tracked over one year. The luminescence of ZGO was recorded both *in vivo* and *ex vivo* to follow the evolution of the optical properties, while quantification by ICP-MS was performed to assess the remaining quantity of ZGO constituting elements in the major organs of accumulation. TEM imaging was also performed to visualize ZGO transformation at the nanoscale. On the other hand, a complete assessment of the potential toxicity was done. Blood count measurements, biochemical analysis, histological examination and determination of gene expression differences of major key metabolisms were carried out.

This comprehensive *in vivo* study provides information on the fate of ZGO and a better understanding of the long-term behavior of such multicomponent inorganic nanoparticles after systemic injection.

Materials & methods

Chemicals were obtained from Sigma-Aldrich, Fluka or Alfa-Aesar. Alpha-methoxy-omega-*N*-hydroxysuccinimide poly(ethylene glycol) MW 5.000 Dalton was bought from Iris Biotech GmbH. Water refers to Millipore water.

ZGO synthesis

$ZnGa_2O_4:Cr^{3+}$ NPs were synthesized by the hydrothermal method developed in our lab.[17] First, gallium nitrate was formed by reacting 8.94 mmol of gallium oxide with 20 mL of concentrated nitric acid (35 wt%) under hydrothermal conditions at 150 °C for 24 hours. Then, a mixture of 0.04 mmol of chromium nitrate and 8.97 mmol of zinc nitrate in 10 mL of water was added to the previous solution of gallium nitrate under vigorous stirring. The resulting solution was adjusted to pH 7.5 with an ammonia solution (30 wt%), stirred for 3 hours at room temperature, and transferred into a 45 mL Teflon-lined stainless-steel autoclave for 24 h at 120 °C. The resulting compound was washed several times with water and ethanol before drying at 60 °C for 2 hours. The dry white powder was finally sintered in air at 750 °C for 5 hours. Hydroxylation was performed by basic wet grinding of the powder (500 mg) for 15 minutes, with a mortar and pestle in 2 mL of 5 mM HCl solution, and overnight vigorous stirring at room temperature at 10 mg mL^{-1} in 5 mM HCl. The hydroxylated ZGO obtained (ZGOOH) NPs with a diameter of 80 nm were first selected from the whole polydisperse colloidal suspension by centrifugation on a SANYO MSE Mistral 1000 at 4500 rpm for 10

minutes. ZGOOH was present in the supernatant (assessed by dynamic light scattering) and was gathered and concentrated.

ZGO functionalization

$ZGONH_2$ NPs were obtained by adding 1 wt% of 3-aminopropyl-triethoxysilane (APTES) to a suspension of ZGOOH NPs at 2.5 mg mL^{-1} in dimethylformamide (DMF). The reaction mixture was sonicated for the first 2 minutes using a Branson Ultrasonic Cleaner 1210 and kept under vigorous stirring for 6 hours at room temperature. The particles were washed from the unreacted APTES by three centrifugation and redispersion steps in DMF. ZGOPEG NPs were obtained by reacting *N*-hydroxysuccinimide activated polyethylene glycol terminated with a methoxy group (MeO-$PEG_{5\,kDa}$-NHS) (50 mg) with $ZGONH_2$ NPs in a 10/1 weight ratio at 2.5 mg mL^{-1} in DMF. To ensure a maximum PEG density, the last functionalization step was performed overnight under vigorous stirring at 90 °C. For this study, ZGOPEG NPs were prepared per 10 mg batch and dried (60 °C, 10 mPa) for storage.

Dynamic light scattering (DLS)

20 µL of each NP suspension (2 mg mL^{-1}) was sampled in triplicate for both size and zeta potential measurements (Nano ZS, Malvern-Instruments). For the hydrodynamic diameter determination, the sample was diluted with 500 µL of Milli-Q water. The presented diameters are a mean of the intensity diameter. For the zeta potential determination, the samples were diluted into 800 µL of 20 mM NaCl solution.

Animals

Balb/cJRj female mice, aged-matched (eight weeks of age, adult) and weight-matched (18–22 g), were purchased from Janvier labs. All experiments involving the mice were approved by French *Comité d'éthique en expérimentation animale* No. 034 and by French Ministry of Research APAFIS#8519-20 16090514387844. The mice were randomly assigned to 7 groups of 6 mice each for experimental purposes. They were maintained in clean facilities with a 12-hour light/dark cycle and received water and food through a semi-barrier system. The NPs were intravenously injected through the tail vein by using insulin syringes (0.2 mL volume containing 10 mg mL^{-1} NP suspension in sterilized 5% glucose solution). The control mice were injected with 5% glucose only. Mouse body weight was monitored every week to control their well-being.

The sacrifice times chosen for this study were distributed over a maximum period of one year after injection of the NPs, namely: 1 h, 1 d, 7 d, 1 m, 3 m, 6 m and 1 year. For all groups, the same protocol was followed. First the animal was anesthetized with gaseous isoflurane and blood was drawn by an intracardiac puncture (EDTA wet syringe) before the animal was sacrificed by cervical dislocation. The liver was first taken to prepare the samples necessary for the different analyses (TEM, histology, and genomics) and then the rest of the liver was divided into three. The spleen, lungs, heart, and kidneys were then collected and placed on a black plate to record the *ex vivo* luminescence of each of the samples. The same samples were kept at −80 °C for ICP-MS analysis.

In vivo luminescence

The *in vivo* luminescence of the NPs of the "1 year" group was monitored at each time corresponding to the time of sacrifice in the study (h1, d1, d7, d30, d90, d180, and d360). The mice were anesthetized with gaseous isoflurane and then placed on the back in groups of three after being shaved. Illumination with an LED with a high-pass filter at 515 nm for 2 min was carried out and the mice were placed under a camera (Optima, Biospace). Signal acquisition was made for 20 min. The mice were under anaesthesia for the duration of the various manipulations. The analysis of the results (Biospace PhotoVision + software) was performed in such a way that a temporal analysis of the signal was carried out over 10 min (step of 10 s), exactly 2 min after the end of the excitation.

The *ex vivo* luminescence acquisition was performed in the same manner as described above. The temporal analysis of the signal is carried out over 10 min (step of 10 s), 2 min after the end of the excitation. Finally, the different organs were placed in pre-tared Eppendorf tubes and were stored at −80 °C before digestion for the ICP-MS analyses.

Blood analysis

After intracardiac puncture, the blood was placed in Eppendorf tubes containing ethylene diamine tetraacetate (EDTA), at a concentration of 10 μL mL^{-1}, to prevent clotting. The samples were placed on ice before analysis. The blood count was taken with MS9 (MS Pharmaceuticals).

After determining the hemogram of each blood sample, it was centrifuged at 4000 rpm at 4 °C for 10 min. The plasma located in the supernatant was removed and then transmitted to the biochemical micro-dosing platform of the Centre for Research on Inflammation (CRI, Bichat Hospital, Paris University). The analyses were carried out using an Olympus AU 400 controller.

Transmission electron microscopy

All steps were performed at room temperature except when otherwise indicated. One cubic millimetre of liver tissue was cut using a razor blade and immersed in a fixative (2% paraformaldehyde, 2.5% glutaraldehyde in 0.1 M sodium cacodylate buffer, pH 7.3) for approximately 3 h. The samples were then washed twice in cacodylate buffer and fixed in the same buffer containing 1% OsO_4 at 4 °C for 1 h. After two washes in cacodylate buffer and a brief rinsing in water, the samples were incubated in 1% aqueous uranyl acetate for 1.5 h in the dark. After a quick rinse in water, dehydration was performed in an increasing series of ethanol (30%, 50%, 70%, and 95%, 15 min each) followed by 100% ethanol (2 × 20 min), ethanol/propylene oxide (1/1) (15 min) and pure propylene oxide (15 min). The liver samples were eventually embedded in Epon resin. Ultra-thin sections (80 nm) were stained using lead citrate and observed at 80 keV in a JEM-100S (Jeol, Croissy-sur-Seine, France) equipped with a 2 × 2k Orius 830 CCD camera (Roper Scientific, Evry, France).

Histology

A section of the large lobe of the liver was cut and immersed in the fixative (4% paraformaldehyde in 0.1 M phosphate buffer) at 4 °C overnight. The pieces of the liver were then dehydrated in ethanol of increasing concentration (70%, 95%, 100%, and 100%, 30 min each) followed by 100% xylene (3 washes, 30 min each) and embedded in paraffin. 4 μm sections were affixed on glass slides, dewaxed, rehydrated and stained with hematoxylin–eosin.

ICP-MS analysis

Organ samples kept at −80 °C were thawed and then weighed directly from the tube before being taken to the ICP-MS platform at Institut de Physique du Globe de Paris (IPGP, PARI platform, Paris University) to perform the mineralization and ion dosage study. The samples were put in 6 mL of distilled concentrated nitric acid (70%) for 24 h at 90 °C using a Digiprep device. The solution was then allowed to cool, and the acid was diluted by adding 44 mL of water. 50 μL of the solution were then taken and placed in 4.95 mL of mQ water for ICP-MS analysis. The instrument (sector-field inductively coupled plasma mass spectrometer, HR-ICP-MS Element II, ThermoScientific) was first tuned to produce maximum sensitivity and stability prior to analysis. Gallium and zinc stock solution (SCP Science, 1 g L^{-1}) were diluted several times in 1% distilled nitric acid to obtain standards for the calibration range (from 10 ng L^{-1} to 10 μg L^{-1}). Then, data were treated as follows: intensities (^{66}Zn & ^{69}Ga) were converted into concentrations using uFREASI (user-FRiendly Elemental dAta proceSsIng).[29]

Total RNA extraction

For each sample, total RNA was isolated from about 10–30 mg (a 3 mm cube) of frozen liver tissue. Before extraction, 10–30 mg of liver tissue was submerged in 600 μL of RNAlater RNA Stabilization Reagent (Qiagen) to protect RNA during storage at −80 °C for 24 h, 48 h or 72 h. Then, liver tissue was homogenized in RNeasy Lysis Buffer (RLT) with 1% mercaptoethanol and one stainless steel bead, and subsequently homogenized twice for 2 min at 30 Hz with the TissueLyser II (Qiagen). Total RNA was extracted from homogenized mouse tissues using an RNeasy Tissue Mini Kit (Qiagen) including on-column DNaseI treatment according to the manufacturer's protocols. Contaminating genomic DNA was degraded by treatment with DNaseI (Qiagen) for 20 min at room temperature according to the instruction manual.

Total RNA was eluted in 30 μL nuclease-free water (Qiagen). RNA purity and quantity were first assessed using NanoDrop (Thermo Fisher). The sample quantity and purity were estimated by measuring the ratios of spectrophotometric absorbance 280 nm/260 nm and 260 nm/230 nm. For a pure RNA sample, these ratios should be between 1.8 and 2.0 and 1.9 and 2.2, respectively. The RNA quality and integrity were further analysed with a

Fragment Analyzer (Agilent Technologies) using Standard Sensitivity RNA Analysis, 15 nt (Agilent Technologies). The RNA Quality Number (RQN) obtained with the Standard Sensitivity RNA Analysis Kit indicates the RNA quality of a sample (RQN > 7 is commonly considered as high-quality RNA). Total RNA was stored at −80 °C before reverse transcription.

Reverse transcription

Total RNA samples were diluted at 200 ng μL^{-1} by adding nuclease-free water. cDNA synthesis was performed using Reverse Transcription Master Mix® from Fluidigm according to the manufacturer's protocol with random primers in a final volume of 5 µL containing 200 ng total RNA (1 µL of Reverse Transcription Master Mix, 1–4 µL of RNA sample and QSF nuclease-free water). Reverse transcription was performed using a Nexus Thermocycler (Eppendorf) following the temperature protocol: 25 °C for 5 min, followed by 30 min at 42 °C and 5 min at 85 °C. cDNA samples were diluted five times by adding 20 µL of low TE buffer [10 mM Tris; 0.1 mM EDTA; pH = 8.0 (TEKNOVA)] and stored at −20 °C before specific target pre-amplification.

Specific target pre-amplification

1.25 µL of each diluted cDNA was used for multiplex pre-amplification with Fluidigm® PreAmp Master Mix at 18 cycles in a total volume of 5 µL containing 1 µL of pre-amplification mastermix, 1.25 µL of cDNA, and 1.25 µL of pooled TaqMan® Gene Expression assays (Life Technologies, Thermo Fisher) with a final concentration of each assay of 180 nM (0.2×) and 1 µL of nuclease-free water. The cDNA samples were subjected to pre-amplification following the temperature protocol: 95 °C for 2 min, followed by 18 cycles at 95 °C for 15 s and 60 °C for 4 min. The pre-amplified cDNAs were diluted 5× by adding 20 µL of low TE buffer (TEKNOVA) and stored at −20 °C before qPCR.

High-throughput real time PCR

Quantitative PCR was performed using the high-throughput platform BioMark™ HD System and the 48.48 GE Dynamic Arrays (Fluidigm). 6 µL of Sample Master Mix (SMM) consisted of 2.7 µL of 5× diluted pre-amplified cDNA, 0.3 µL of 20× GE Sample Loading Reagent (Fluidigm) and 3 µL of TaqMan® Gene Expression PCR Master Mix (Life Technologies, Thermo Fisher). Each 6 µL Master Mix Assay (MMA) consisted of 3 µL of TaqMan® Gene Expression assay 20× (Life Technologies, Thermo Fisher) and 3 µL of 2× Assay Loading Reagent (Fluidigm). 5 µL of each SMM and each MMA premix were added to the dedicated wells. The samples and assays were mixed inside the chip using an MX IFC controller (Fluidigm). The parameters of the thermocycler were set with ROX as a passive reference and single probe FAM-MGB as a fluorescence detector.

Thermal conditions for qPCR were 25 °C for 30 min and 70 °C for 60 min for thermal mix; 50 °C for 2 min and 95 °C for 10 min for hot start; and 40 cycles at 95 °C for 15 s and 60 °C for 1 min. To determine the quantification cycle Cq, data were processed with an automatic threshold for each assay, with linear derivative baseline correction using BioMark Real-Time PCR Analysis Software 4.0.1 (Fluidigm). The quality threshold was set at a default setting of 0.65.

Data analysis

Data analysis was performed using the programming software R (version 3.6.3) to measure the relative gene expression using the comparative Cq method of Livak *et al.* (2001),[47] after normalization with Hprt, Actb, Gapdh, B2m and Canx reference genes. Gene expression in log fold change was calculated as follows: $R = 2 - \Delta\Delta Cq$, where $\Delta\Delta Cq$ is equal to the difference between ΔCq for the genes of interest under control and experimental conditions [$\Delta\Delta Cq = \Delta Cq$ treated $- \Delta Cq$ control = (Cq GOI, treated − Cq ref, treated) − (Cq GOI, control − Cq ref, control)] where GOI designates the gene of interest, and ref the reference genes. As several reference genes were used here, the mean Cq of the five reference genes was considered. Principal component analysis reveals a batch effect between the different time points, which was thus corrected using ComBat function of the sva package. The significance of differential gene expression was calculated from log fold change values using Welch's *t*-test with *t*.test function, and a Bonferroni correction for multiple testing using *p*.adjust function. The expression heatmap was generated using pheatmap package and function.

Results and discussion

To carry out this *in vivo* study, 100 mg of ZGOOH and 100 mg of ZGOPEG were prepared (Table S1†). It is interesting to note that this same batch of ZGO has been used in a previous study to determine its degradation in artificial lysosomal fluid.[26] The PEGylated particles used in this study were prepared in 10 batches of 10 mg each, which were then pooled. In the end, approximately 100 mg of ZGOPEG were obtained with an average hydrodynamic diameter of 138 ± 20 nm and a zeta-potential of −1.69 ± 1.38 mV. Similarly, 10 batches of 10 mg of ZGOOH were prepared before use, with an average hydrodynamic diameter of 88 ± 8 nm and a zeta-potential of 24.1 ± 2.90 mV. The samples were characterized after UV and visible light excitation, to control their optical properties for the study.[26] The mice were injected with a dose of 100 mg kg^{-1} (approximately 2 mg of NPs/200 μL per mouse). This dose was determined in previous work[13] to obtain a sufficient intensity of the light signal collected from the injected ZGO. A control group of mice, injected with the same volume of injection medium but without NPs, was also used for each time-point. The sacrifice time-points were distributed over a period of one year after injection of the NPs, namely: 1 hour (t0 or h1), 1 day (d1), d7, d30, d90, d180 and d360.

Luminescence properties of ZGO diminish after one month in the body

The *in vivo* luminescence properties were monitored after visible light excitation at the different time-points (Fig. 1A). The evolution of the luminescence signal was followed in the same mice (n = 6) kept alive for one year after injection of ZGOOH and ZGOPEG. As previously described, a rapid accumulation in the liver is observed for ZGOOHs unlike ZGOPEGs that are stealthier in the short time due to their polymer coating (Fig. S1†). Nonetheless, it is visible that one day after injection the recorded light signal distribution is almost similar for both coatings. At longer time-points, from one month to one year, we observe a common decrease in the luminescence signal in each group. This loss of luminescence signal over time can be attributed to the excretion of ZGOs out of the organ or/and to their *in situ* degradation and loss of luminescence properties. This decrease of luminescence signals could be also due to the physiological tissue evolution such as accumulation of adipose tissues due to aging of the mice. This adipose tissue layer could then increase the depth at which the NPs reside and thus decrease their sensitivity towards the excitation source. This assumption alone cannot explain the decrease at a short time-point. To be independent of such an effect, the *ex vivo* luminescence of each organ was examined (Fig. 1C and E) and quantified (Fig. 1B and D). Interestingly, luminescence was observed in the lungs, which was difficult to differentiate from the liver *in vivo* with ZGOOH injected mice (Fig. 1A). This observation can be explained by the surface charge of ZGOOH (~24 mV), which has already been indicated as responsible for a transient targeting of the lungs for other types of nanoparticles.[30] In contrast, the luminescence in the liver first increased at day 1 and then decreased over one year (Fig. 1B). Indeed, the quantification shows a rapid increase from 10 to 23 counts per mg between t0 and d1, and then a decrease to 3 counts per mg at d7. In contrast to the liver, the luminescence continuously decreased in the spleen reaching control values after one month (approximately 0.5 count per mg, Fig. S2†). This could indicate a transient biological process, causing ZGOOH to circulate from the blood system to the spleen and liver and then be stored in the liver for months.[31] Indeed, the signal collected in the liver at d1 corresponds to approximately 83% of the luminescence collected at t0 in the different organs. Finally, no light signal was observed in the kidneys, the heart, or the blood, matching the control group values (Fig. S2†).

Fig. 1

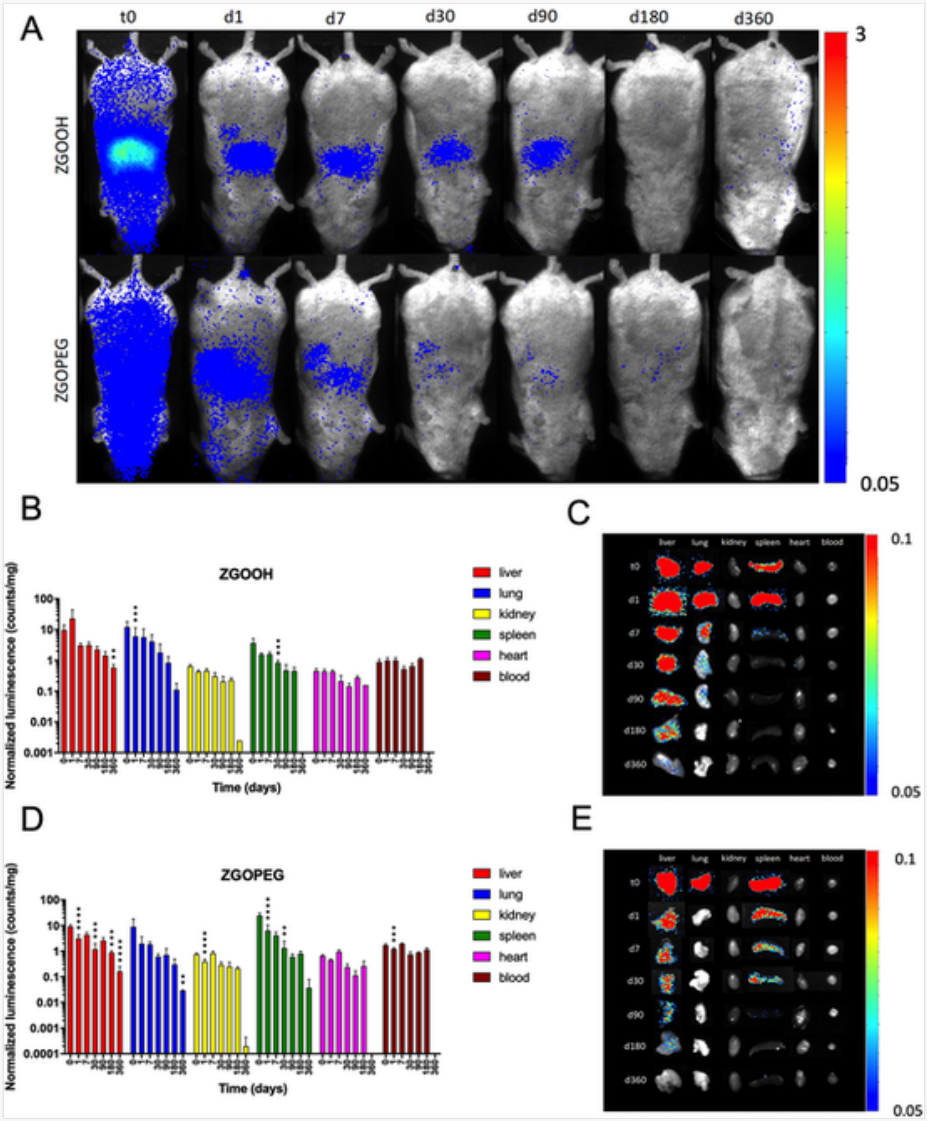

(A) *In vivo* luminescence evolution after injection. The mice of the one-year group were monitored at each time-point on their back and exposed to visible light excitation (above 600 nm) for 2 min. Photon counts were recorded for 10 min, exactly 2 min after the end of the excitation. The false colour scale goes from 0.05 (blue) to 3 (red) counts per min. Quantification of the maximum intensity of ZGOOH (B) and ZGOPEG (D) luminescence on *ex vivo* samples (C and E, respectively; the false color scale goes from 0.05 (blue) to 0.1 (red) counts per min). The presented values correspond to the first ten seconds of the luminescence decays recorded, for each organ. Statistical differences between anterior adjacent time-points within each group were assessed using multiple *t*-test analysis. Discovery using the two-stage linear step-up procedure of Benjamini, Krieger and Yekutieli, with $Q = 1\%$. Each row was analysed individually, without assuming a consistent SD (****: $p < 0.0001$; ***: $p < 0.001$; **: $p < 0.01$; *: $p < 0.1$; ns: $p > 0.1$). The error bars represent the standard deviation ($n = 6$).

After injection of ZGOPEGs (Fig. 1E), the maximum luminescence signal was observed in the liver, lungs, and spleen soon after 1 h. Nevertheless, a strong diminution of the signal intensity is observed between t0 and d1, corresponding to a 66%, 78%, and 74% decrease for the liver, lungs, and spleen respectively (Fig. 1D). These observations are consistent with what was observed in a previous study,[17] while giving more insights concerning the long-term behaviour. The difference of behaviour observed between ZGOOH and ZGOPEG could indicate a heterogeneity in terms of tissue uptake. Similarly, to ZGOOH, no luminescence was observed in the kidneys and the heart.

Overall, the luminescence signal drastically decreased over time in the lungs, liver, and spleen without signal transfer in other organs or blood. These observations are consistent with previous studies highlighting a loss of luminescence 2 months postinjection.[28] This suggests that ZGO nanoparticles, in case they are still in the organs, can lose their structural integrity or interact with the biological environment in such a way that it affects their luminescence properties.[32] Nevertheless, *ex vivo* luminescence signals in the liver are still observed one year postinjection for ZGOOH and 6 months postinjection for ZGOPEG.

Elemental components of ZGO persist in the body over one year

To quantify the presence of the elements constituting ZGO NPs in various organs, ICP-MS analyses were carried out. Each major organ (liver, kidneys, spleen, lungs, and heart), as well as blood samples, were collected and digested in hot concentrated nitric acid. The main elements of ZGOs (Zn, 24.32% in mass and Ga, 51.87% in mass)[26] were assayed thanks to the high sensitivity (<1 ppt) of the ICP-MS. Chromium III was not quantified due to the low doping concentration (0.5% in mol). Each Zn and Ga concentration obtained was normalized to the mass of the organ sample and calculated as the percentage of injected dose (nominal injection dose of 1.037 mg of Ga and 0.486 mg of zinc in total). Due to the high content of endogenous Zn as seen in the control group (Fig. S3†), calculations using only Ga quantification were focused on (Fig. 2).

Fig. 2

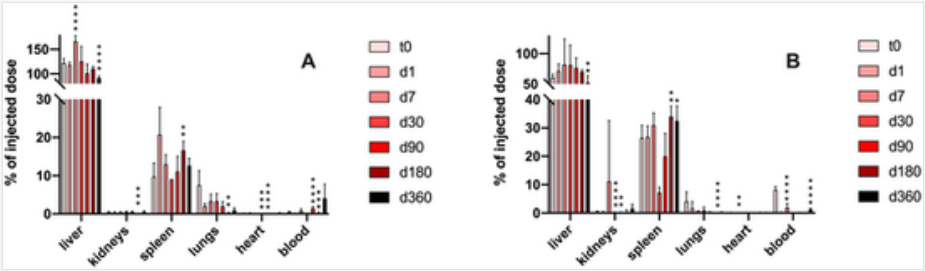

ZGOOH (A) and ZGOPEG (B) ICP-MS quantification in each organ over time. The percentage of injected dose has been calculated for the gallium content quantification regarding the theoretical original injected amount. The error bars represent the standard deviation (n = 6). Statistical differences between anterior adjacent time-points within each group were assessed using multiple t-test analysis. Discovery using the two-stage linear step-up procedure of Benjamini, Krieger and Yekutieli, with Q = 1%. Each row was analysed individually, without assuming a consistent SD (****: $p < 0.0001$; ***: $p < 0.001$; **: $p < 0.01$; *: $p < 0.1$; ns: $p > 0.1$). Number of t tests: 6.

Almost the total injected dose can be found in the liver and spleen, both for ZGOOH (Fig. 2A) and ZGOPEG (Fig. 2B) NPs. In line with luminescence data at the time-points before 1 month, we observe that the gallium concentration is higher in spleen for ZGOPEG in comparison with ZGOOH. Also consistent with the luminescence, a small portion of Ga (or Zn, Fig. S3A & B †) was found in the lungs one hour after injection (7.5% for ZGOOH and 4.1% for ZGOPEG) but decreased over time reaching control values from 1 month to 3 months (Fig. S3†). In the same manner, a significant increase of gallium and zinc content in the liver is observed for ZGOOH injected mice between d1 and d7. Overall, the most striking result is that the total amount of Ga and Zn retrieved in organs did not decrease substantially up to one year, unlike the luminescence signal that diminished over the first month post-administration. Quantitatively, for ZGOOH, the liver retained almost the totality of the injected dose of Ga and Zn while around 10 ± 4% was kept in the spleen. ZGOPEG presents around 75 ± 10% of the dose in the liver and 25 ± 5% in the spleen. By considering the one-year time point, an absence of Ga elimination from the body can be highlighted, with a 115 ± 10% dose detected for ZGOOH and 88 ± 16% for ZGOPEG with marked persistence in the liver and spleen. In detail, we observed a very slow and slight diminution (about 30%) of Ga liver concentration from 1 month to 1 year for both ZGOOH and ZGOPEG. In the spleen, the Ga concentration shows a biphasic profile with a diminution at intermediate time-points (day 30 and day 90) and an increase at longer time points (day 180 and day 360), which could indicate a recirculation of Ga between the liver and spleen, both organs sequestrating almost the total injected dose after one year.

Therefore, the decrease of the luminescence probably cannot be attributed to the elimination of the NP components. To assess this hypothesis, correlation statistic tests had been performed between the luminescence and ICP quantification. It must be noted that both analyses were performed on the same organ sample. Interestingly, a strong correlation was found between both quantifications (Fig. S4†). As expected, significant results were obtained principally on the organs concentrated in ZGO, but also on Ga quantification, less disturbed by the endogenous metal content than Zn. In a general manner, it has been shown that the observed decrease of luminescence was directly linked to the slight decrease of ZGO composing elements in the corresponding organs. Nevertheless, the slow decrease of NP content inside the organs cannot explain by itself the strong decrease in luminescence intensities.

Moreover, the ratio of Zn over Ga contents in the liver and spleen did not vary over time and is close to the initial value of the injected particles (2/1 mass ratio in Ga/Zn) (Fig. S3E & F †). This reveals a persistent colocalization of the

particle components in the tissues.

We thus interrogated the structural integrity of NPs by TEM imaging to gain better insight of their fate.

Intracellular aggregates of ZGO NPs persist in the liver for at least a year

To monitor the integrity of ZGOs after injection, pieces of the liver were fixed and embedded in resin for TEM observations. All images show that ZGOs are stored in vesicles inside the cytoplasm that are presumably lysosomes. This organelle is known to be involved in the degradation of proteins and of inorganic nanoparticles, because of its acid content (pH about 4.5), its protein content[33] or its ability to generate highly reactive oxidative species.[34] Hence, we wondered whether this lysosomal content could affect the integrity of ZGOs over time. The images obtained (Fig. 3) clearly indicate that many intact ZGO NPs were still observed over long periods of time, both for ZGOPEG and ZGOOH.

Fig. 3

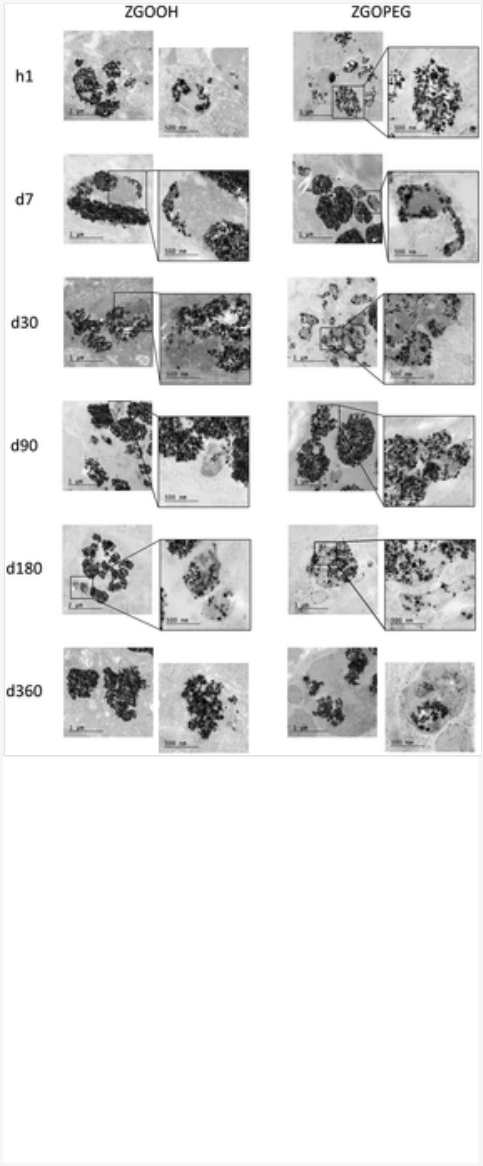

Observation by transmission electron microscopy of hepatic tissues at different sacrifice times postinjection.

Large aggregates of ZGO were observed in the lysosomes of liver cells as early as an hour after injection and the lysosomal accumulation tends to be amplified over time. To quantify this phenomenon, image processing was carried out on TEM images, by measuring the area of these aggregates. A significant increase of the area of these aggregates was measured over time (Fig. S5†). This phenomenon might be explained by the management of nanoparticles by Kupffer cells. Indeed, the latter have a lifespan of several weeks.[35] Thus, the NPs could be released when the cells die and recovered by new viable Kupffer cells or other cell types, thus creating a concentration phenomenon, which has

already been observed for skin macrophages.[36] Overall the presence of micrometric aggregates of intact NPs within the intracellular compartment together with the elemental persistence of Ga and Zn in the liver up to a year post-injection, the latter time-points of the experiment, suggest that ZGO NPs, whatever their initial coating, are barely not degraded by the organism at this dosage over one year. To gain further insights into the degradation process, images were processed to get ZGO size distribution over the time (n > 100, Fig. S6†). The median diameter of ZGOOH and ZGOPEG NPs decreased respectively by 9% (from 46 to 42 nm) between t0 and d30 and 15% (from 46 to 39 nm) between t0 and d7 and remained unchanged thereafter up to d180. This confirms that the degradation of NPs is very limited over this period. The increase in the median diameter between d180 and d360 for ZGOOH and ZGOPEG might result from the fact that the smallest NPs have been completely degraded, thus skewing the size distribution towards higher values.

Altogether, TEM results confirm the biopersistence behaviour of the ZGO in the liver up to one year following injection. To investigate the biological impact of the one-year ZGO biopersistence, a complete toxicity evaluation was conducted.

Biopersistence of ZGO NPs does not induce toxicity in the long-term

As seen above, ZGO NPs are not eliminated after their accumulation in the liver and spleen in the form of micrometric intracellular aggregates that are still observed one year after injection. The decrease in luminescence properties observed previously could thus be due to their increasing state of agglomeration and also the loss of the dopant Cr^{3+}. In both cases, such intracellular processing could cause long term toxicity. The accumulation and persistence of NPs in the intracellular lysosomes can affect the metabolism of the cells by causing lysosomal stress and disruption, or by impeding the physiological protein degradation in these compartments. If NPs are taken up by macrophages, circulating or resident, the production of free radicals could cause damage at the cellular level and lead to inflammation.[37] Likewise, if ZGOs reach the lysosomal compartments without being degraded, toxicity could be induced, as observed in diseases linked to a loss of lysosome activity.[38] Indeed, lysosome disruption leads to the cytosolic release of degradation enzymes that induce necrosis.[39] Thus, a complete evaluation of the toxicity induced by the long-term intracellular persistence of ZGOs must be carried out in order to know whether lysosomal accumulation can have a biological impact.

Mouse weight was first monitored every two days up to a week after injection and then every month until the date of sacrifice (Fig. S7†). No significant difference was observed between the control group and the groups that received the 2 mg injection of ZGO NPs. This follow-up allows us to conclude that the biopersistence of ZGO NPs did not induce any deleterious effects affecting the body mass.

Then, the plasma was extracted from each of the blood samples, and some biomarkers were selected and assayed. We chose blood markers involved in the metabolism of the liver, spleen and kidneys that could reflect the damage in these organs. First, we did not observe major changes in two transaminases, alanine aminotransferase (ALAT) and aspartate aminotransferase (ASAT) (Fig. 4A & B). Only a slight decrease is observed one-day after injection. It is interesting to note that ASAT takes part in the urea cycle, which results in the production of creatinine. It is therefore not surprising to observe a stable creatinine concentration over time and conditions (Fig. 4C), which indicates that this key factor of kidney metabolism is not affected by the biopersistence of ZGO NPs. Finally, ferritin (Fig. 4D), which supports the storage of more than a thousand iron(III) ions per protein,[40] as well as transferrin (Fig. 4E), providing iron support to its storage site, have been studied. Interest was focused on these proteins because a comparison was made between the Ga^{3+} and Fe^{3+} ions, due to their charge and their similar atomic radii.[41] Thus, a release of gallium ions could eventually have an impact on the concentrations of these two proteins. A small increase in ferritin was observed at d180 for both groups, highlighting a late transformation of ZGO, correlated with the NP's content decrease in the liver observed by ICP quantification. The concentrations of albumin (Fig. 4F), as well as that of total plasma proteins (Fig. 4G), also show a few significant differences between the groups, which indicates the absence of liver or inflammatory diseases. Moreover, blood microanalysis was performed at each time-point to quantify white blood cells (WBC), platelets (PLT), lymphocytes (LPC), monocytes (MNC) and mean corpuscular volume (MCV) (Fig. 4H–L). Complementary dosages are shown in Fig. S8.† This information gives an overview of the general condition of the animal and the onset of inflammation or haemolysis. Remarkably we did not observe large significant differences as

compared to the control for any of the time-points, with the exception of the first one, at one hour post-injection. The injection of ZGO seems to cause a slight and transient inflammation. Similar effects have already been reported[22] in a short term study indicating a greater response to the injection of ZGOOH compared to that of ZGOPEG. However, this inflammation was not observed for the longer time-points of the present study, thus confirming a short-term effect caused by the contact between the ZGOOH and the blood plasma after injection, as has already been described.[42]

Fig. 4

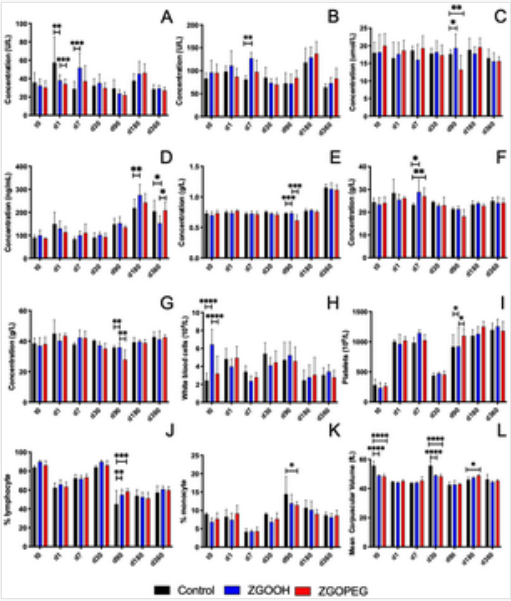

Monitoring of different biochemical markers and blood analysis of mice after injection of ZGOOH (blue), ZGOPEG (red) and the control group (black). The concentrations of alanine aminotransferase or ALAT (A), aspartate aminotransferase or ASAT (B), creatinine (C), ferritin (D), transferritine (E), albumin (F) and total protein (G) were examined. The rate of white blood cells (H), the platelet concentration (I), the percentage of lymphocytes (J), the percentage of monocytes (K) and the average globular volume (L) were examined. Statistical differences with the control group at each time-point were assessed by using two-way ANOVA analysis (****: $p < 0.0001$; ***: $p < 0.001$; **: $p < 0.01$; *: $p < 0.1$; ns: $p > 0.1$). The error bars represent the standard deviation ($n = 6$).

Overall, ZGO NPs do not induce any effects on serum markers or blood components at any time from one day post-administration of the single dose, thus establishing that ZGOs, with or without PEGylation, do not cause major liver or nephrotic suffering. These observations are consistent with previous studies highlighting an absence of toxicity even with high doses, up to 6 months postinjection.[27]

Finally, in complement to hepatic and blood markers, histological examinations of the liver tissue have been performed to reveal if the accumulation and persistence of ZGOs in this organ could induce tissue damage, sites of inflammation, or lesions. No histopathological anomalies could be observed regardless of the time-point after injection (Fig. 5). Only a few sites of inflammation were observed (data not shown). These sporadic observations did not, however, highlight a systematic chronic inflammation which is repeatedly present. Overall, no sign of chronic toxicity of ZGO biopersistence was observed in the long term in the liver tissue or in blood analysis. Similar observations have already been made on the spleen, kidneys and lungs for a shorter term.[27]

Fig. 5

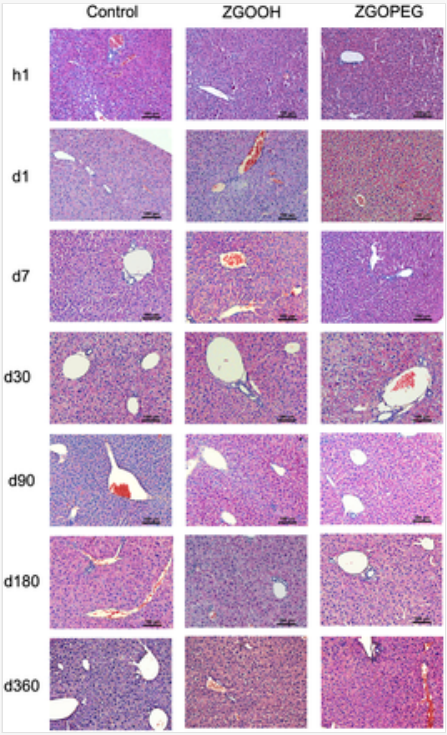

Monitoring of liver tissue over time by histology after haematoxylin–eosin staining ($N = 2$, 5 photographs per slide).

Gene expression profile of the liver tissue is barely affected by the biopersistence of ZGO NPs at long-term

To study in depth the potential impact of a one-year persistence of ZGO in the body, we sought to investigate whether the expression of certain key genes could be affected. Again, we focused on liver tissue because it accumulates a major part of ZGOs. Seven different "families" of genes were chosen, for a total of 31 genes studied.

First, particular interest was focused on the genes encoding for metal ion transport and storage. Zinc ions are mostly stored by metallothioneins, which are encoded by four coding genes (Mt1 to 4). These proteins have a high content of cysteine, which enables them to complex monovalent and divalent metal ions.[35] The family of metallothioneins thus participate in the detoxification of heavy metals. In contrast to zinc, gallium is present in a very small amount in the body. However, thanks to studies on the role of Ga(III) in the treatment of lymphoma,[41] it has been highlighted that metallothioneins Mt2, Mt3 and Mtf1 showed overexpression in the presence of Ga(III). In the same way, the Metal Regulatory Transcription Factor 1 (Mtf1) gene was investigated, as it controls metallothionein expression and metal ion transporters.[43] We also focused on the known transporters of ZGO's constituting elements. As the role of zinc in the body is well known and studied, the Solute Carrier Family (Slc) was highlighted. This family of genes has more than 400 members divided into 65 groups. They mainly code for transmembrane proteins ensuring the passage of various compounds, organic or inorganic, charged or not.[44] Subgroups 30 and 39 were highlighted for their role with respect to zinc.[45] Moreover, Slc30a1 (also called Zinc Transporter 1, ZnT1) has also been shown to be up-regulated after exposure to gallium.[41] Altogether, the expression of twelve specific genes has been monitored to assess the possible impact of zinc or gallium overload in the liver.

Beside the genes involved in the metabolism of metal ions, attention was paid to different signalling pathways, making it possible to refine the assessment of the toxicity of ZGOs in the long-term. As these signalling pathways are very complex, involving several hundred genes, linked together by activation/inhibition phenomena, a choice of key genes of metabolic activity has been made. Therefore, genes related to oxidative stress, immune responses and inflammation, apoptosis and DNA damage/repair have been studied. Five reference genes (Hprt, Gapdh, CanX, B2m and Actb) have also been selected after pair-wise correlation analysis because of their stability according to treatments and their duration.[46] They have been used to normalize the results by the Livak method.[47]

Among the 31 genes analysed, only 2 showed significant differences in expression at any time-point of the study. A summary of the results obtained is presented in the heat map in Fig. 6A. We can distinguish a response at short term

that slightly differs for ZGOOH and ZGOPEG and a response at long term that appears from one month. Regarding the short-term response, the interferon pathway represented by the Tnf gene is under-expressed at 1 hour and day 1 and then over-expressed after one week. This gene, from the cytokine family, plays a role in recruiting and activating macrophages and lymphocytes at the site of local inflammation.[48] This phenomenon seems to be more important for ZGOPEG. Similar observations were made following the administration of PEGylated liposomes.[49] Studies have indeed demonstrated the immunogenic properties of the PEG itself, leading to faster elimination of NPs after a second injection.[50] In the same way, Fos is also overexpressed 1 h postinjection, implying an increase of apoptosis in the liver. This short-term response was observed before for other nanoparticles, being non-specific to the materials.[34]

Fig. 6

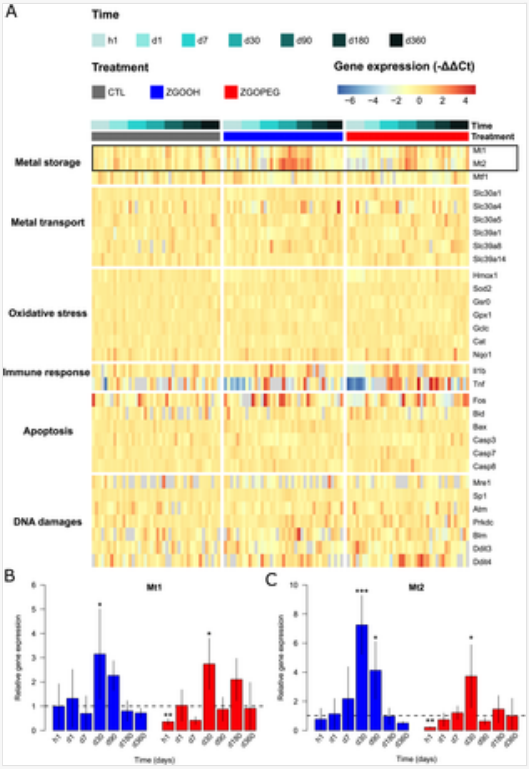

Heatmap of the gene expression in log fold change across conditions (A). The black box highlights the two genes that are significantly differentially expressed between the control conditions and at least one of the treated conditions. The relative expression of these two genes, which are Mt1 and Mt2, is displayed in B and C, respectively. Error bars represent the standard deviation ($3 \leq n \leq 6$). The black dotted lines indicate the normalized expression level of the control conditions. p-values were calculated by Welch's t-test with Bonferroni correction. * $p < 0.5$, ** $p < 0.1$, *** $p < 0.01$.

Interestingly, the overexpression of the Mt1 and Mt2 genes, coding for heavy metal transporter proteins as well as antioxidants, is observed (Fig. 6B and C). Indeed, an activation of these transporters is seen between one month and three months for both ZGO groups. This could be due to the start of NP degradation leading to the processing of metal ions by metallothioneins which occurred a few months after injection, and more importantly for ZGOOH than ZGOPEG. These results are consistent with what has been published with an *in vitro* degradation model,[26] with a faster degradation of ZGOOH than ZGOPEG. Nevertheless, we are unable to establish why the over-expression of metallothioneins stopped over time. It is interesting to note that Mt1 and Mt2 activation parallels with changes in creatinine, total plasma proteins, platelets, and lymphocyte contents (Fig. 4).

In a general manner, these results are consistent with the other techniques used to assess the toxicity of ZGOs, showing no effect on the oxidative stress, DNA damage/repair or metabolism pathways.

Thus, the gene expression profile has been able to highlight a slight short-term response to ZGOPEG, and to a lesser extent to ZGOOH, followed by a transient activation of metal transporters one month postinjection, without any sign of long-term toxicity.

Conclusions

This study provides the first comprehensive evaluation of the long-term fate of ZGO persistent luminescence nanoparticles with two different surface states up to one year after their single systemic injection in mice. The evolution of the luminescence was monitored and it indicates a rapid drop in the *in vivo* signal as early as a week after injection, with a slower diminution on *ex vivo* samples. Observations by electron microscopy revealed an increasing and significant intracellular accumulation of ZGO NP aggregates in liver cells (principally Kupffer cells), while elemental analysis by ICP-MS did not show a significant decrease in the amount of ZGO's constituting elements, Zn and Ga, in the liver and spleen, which are the main organs of accumulation of those nanoparticles. Therefore, it can be assumed that most NPs are not degraded, nor eliminated after their accumulation in the reticulo-endothelial surface, albeit they lose their luminescence properties. A complete analysis of the toxicity related to the biopersistence of ZGO was assessed over one year, combining the animal's weight, key haematological and metabolic markers, and histological observation of liver tissue. Finally, a study of the level of expression of 31 genes linked to different metabolic reactions, including metal iron processing, was carried out. The combined results did not show any form of ZGO toxicity, with the exception of a slight inflammatory reaction at the first hours following injection. This study thus demonstrated the non-degradation of the ZGO NPs after storage, mainly in the liver and spleen, without causing major toxicity. Therefore, this safe imaging probe has been proven to be a relevant candidate for preclinical studies, allowing long term use without any disturbance of the general metabolism. Meanwhile, an increase in the signal intensity to dose ratio, as well as a longer circulation time in blood, must be improved for a key role in clinical trials.[51]

Author contributions

T. Lécuyer was the principal contributor on the experimental work. J. Seguin brought expertise with *in vivo* imaging. M. Delagrange and B. Ducos brought expertise with genetic experiments while A. Balfourier ensured data analyses. P. Burckel and M. Tharaud oversaw the ICP-MS measurements. R. Lai-Kuen, V. Mignon and B. Saubaméa helped with the preparation and visualization of samples for histology and electron microscopy. Finally, D. Scherman and N. Mignet brought funding to support the project while C. Richard and F. Gazeau overviewed the study.

Conflicts of interest

There are no conflicts to declare.

Acknowledgements

This work was supported by French Research Agency (ANR-14-CE08-0016-01) and by the European Union (NanoTBTech project, Horizon 2020 FET Open, grant agreement no 801305). The authors would like to acknowledge the support by the IPGP multidisciplinary program PARI and by Région Île-de-France SESAME (Grant No. 12015908). The gene expression analysis was carried out on the high throughput qPCR-HD-Genomic Paris Centre core facility and was supported by grants from the Région Île-de-France.

References

References can be edited in the panel that appears to the right when you click on a reference.

1 D. Jaque, C. Richard, B. Viana, K. Soga, X. Liu and J. G. Solé, *Adv. Opt. Photonics*, 2016, **8**, 1–103.

2 T. L. Doane and C. Burda, *Chem. Soc. Rev.*, 2012, **41**, 2885–2911.

3 S. M. Janib, A. S. Moses and J. A. MacKay, *Adv. Drug Delivery Rev.*, 2010, **62**, 1052–1063.

4 Z.-Y. Chen, Y.-X. Wang, Y. Lin, J.-S. Zhang, F. Yang, Q.-L. Zhou and Y.-Y. Liao, Advance of Molecular Imaging Technology and Targeted Imaging Agent in Imaging and Therapy, https://www.hindawi.com/journals/bmri/2014/819324/ , (accessed May 4, 2020)

Q. Miao, C. Xie, X. Zhen, Y. Lyu, H. Duan, X. Liu, J. V. Jokerst and K. Pu, *Nat. Biotechnol.*, 2017, **35**, 1102–1110.

6 Y. Jiang and K. Pu, *Chem. Rev.*, 2021, **121**, 13086–13131.

7 B. R. Smith and S. S. Gambhir, *Chem. Rev.*, 2017, **117**, 901–986.

8 J. Xu and S. Tanabe, *J. Lumin.*, 2019, **205**, 581–620.

9 T. Lécuyer, E. Teston, G. Ramirez-Garcia, T. Maldiney, B. Viana, J. Seguin, N. Mignet, D. Scherman and C. Richard, *Theranostics*, 2016, **6**, 2488–2524.

10 A. Benayas, E. Hemmer, G. Hong and D. Jaque, Near Infrared-Emitting Nanoparticles for Biomedical Applications, Springer Nature, 2020

11 J. Liu, T. Lécuyer, J. Seguin, N. Mignet, D. Scherman, B. Viana and C. Richard, *Adv. Drug Delivery Rev.*, n.d., DOI: 10.1016/j.addr.2018.10.015.

12 Q. le M. de Chermont, C. Richard, J. Seguin, C. Chanéac, M. Bessodes and D. Scherman, in Colloidal Quantum Dots for Biomedical Applications IV, International Society for Optics and Photonics, 2009, vol. 7189, p. 71890B

13 A. S. Paterson, B. Raja, G. Garvey, A. Kolhatkar, A. E. V. Hagström, K. Kourentzi, T. R. Lee and R. C. Willson, *Anal. Chem.*, 2014, **86**, 9481–9488.

14 B.-Y. Wu, H.-F. Wang, J.-T. Chen and X.-P. Yan, *J. Am. Chem. Soc.*, 2011, **133**, 686–688.

15 G. Ramírez-García, M. Martínez-Alfaro, F. d'Orlyé, F. Bedioui, N. Mignet, A. Varenne, S. Gutiérrez-Granados and C. Richard, *Int. J. Pharm.*, 2017, **532**, 696–703.

16 E. Teston, T. Maldiney, I. Marangon, J. Volatron, Y. Lalatonne, L. Motte, C. Boisson-Vidal, G. Autret, O. Clément, D. Scherman, F. Gazeau and C. Richard, *Small*, 2018, **14**, 1800020.

17 T. Maldiney, A. Bessière, J. Seguin, E. Teston, S. K. Sharma, B. Viana, A. J. J. Bos, P. Dorenbos, M. Bessodes, D. Gourier, D. Scherman and C. Richard, *Nat. Mater.*, 2014, **13**, 418–426.

18 E. Teston, S. Richard, T. Maldiney, N. Lièvre, G. Y. Wang, L. Motte, C. Richard and Y. Lalatonne, *Chem. – Eur. J.*, 2015, **21**, 7350–7354.

19 T. Maldiney, M. Rémond, M. Bessodes, D. Scherman and C. Richard, *J. Mater. Chem. B*, 2015, **3**, 4009–4016.

20 T. Lécuyer, N. Bia, P. Burckel, C. Loubat, A. Graillot, J. Seguin, Y. Corvis, J. Liu, L. Valéro, D. Scherman, N. Mignet and C. Richard, *Nanoscale*, 2022.

21 S.-J. Choi, J. K. Lee, J. Jeong and J.-H. Choy, *Mol. Cell. Toxicol.*, 2013, **9**, 205–210.

22 J. Liu, M. Yu, C. Zhou and J. Zheng, *Mater. Today*, 2013, **16**, 477–486.

23 Balasubramanian, T. Sravanthi and V. Sujitha, *Int. J. Pharm. Sci. Drug Res.*, 2015, 129–137.

24 P. Foroozandeh and A. A. Aziz, *Nanoscale Res. Lett.*, 2018, **13**, 339.

25 N. Feliu, D. Docter, M. Heine, P. del Pino, S. Ashraf, J. Kolosnjaj-Tabi, P. Macchiarini, P. Nielsen, D. Alloyeau, F. Gazeau, R. H. Stauber and W. J. Parak, *Chem. Soc. Rev.*, 2016, **45**, 2440–2457.

T. Lécuyer, M.-A. Durand, J. Volatron, M. Desmau, R. Lai-Kuen, Y. Corvis, J. Seguin, G. Wang, D. Alloyeau, D. Scherman, N. Mignet, F. Gazeau and C. Richard, *Nanoscale*, 2020, **12**, 1967–1974.

27 G. Ramírez-García, S. Gutiérrez-Granados, M. A. Gallegos-Corona, L. Palma-Tirado, F. d'Orlyé, A. Varenne, N. Mignet, C. Richard and M. Martínez-Alfaro, *Int. J. Pharm.*, 2017, **532**, 686–695.

28 X. Sun, J. Shi, X. Fu, Y. Yang and H. Zhang, *Sci. Rep.*, 2018, **8**, 1–11.

29 M. Tharaud, S. Gardoll, O. Khelifi, M. F. Benedetti and Y. Sivry, *Microchem. J.*, 2015, **121**, 32–40.

30 Q. le M. de Chermont, C. Chanéac, J. Seguin, F. Pellé, S. Maîtrejean, J.-P. Jolivet, D. Gourier, M. Bessodes and D. Scherman, *Proc. Natl. Acad. Sci. U. S. A.*, 2007, **104**, 9266–9271.

31 J. Kolosnjaj-Tabi, Y. Javed, L. Lartigue, J. Volatron, D. Elgrabli, I. Marangon, G. Pugliese, B. Caron, A. Figuerola, N. Luciani, T. Pellegrino, D. Alloyeau and F. Gazeau, *ACS Nano*, 2015, **9**, 7925–7939.

32 A. S. Susha, A. M. Javier, W. J. Parak and A. L. Rogach, *Colloids Surf., A*, 2006, **281**, 40–43.

33 J. Volatron, F. Carn, J. Kolosnjaj-Tabi, Y. Javed, Q. L. Vuong, Y. Gossuin, C. Ménager, N. Luciani, G. Charron, M. Hémadi, D. Alloyeau and F. Gazeau, *Small*, 2017, **13**, 1602030.

34 A. Balfourier, N. Luciani, G. Wang, G. Lelong, O. Ersen, A. Khelfa, D. Alloyeau, F. Gazeau and F. Carn, *Proc. Natl. Acad. Sci. U. S. A.*, 2020, **117**, 103–113.

35 A. T. Nguyen-Lefebvre and A. Horuzsko, *J. Enzymol. Metab*, n.d..

36 Unveiling skin macrophage dynamics explains both tattoo persistence and strenuous removal, *J. Exp. Med*., https://rupress.org/jem/article/215/4/1115/42419/Unveiling-skin-macrophage-dynamics-explains-both, (accessed October 7, 2020)

37 B. K. Gaiser, S. Hirn, A. Kermanizadeh, N. Kanase, K. Fytianos, A. Wenk, N. Haberl, A. Brunelli, W. G. Kreyling and V. Stone, *Toxicol. Sci.*, 2013, **131**, 537–547.

38 A. Vellodi, *Br. J. Haematol.*, 2005, **128**, 413–431.

39 M. E. Guicciardi and G. J. Gores, *Cell Cycle*, 2013, **12**, 1995–1995.

40 E. C. Theil, *Annu. Rev. Nutr.*, 2004, **24**, 327–343.

41 C. R. Chitambar, *Biochim. Biophys. Acta, Mol. Cell Res.*, 2016, **1863**, 2044–2053.

42 Y. Jiang, Y. Li, C. Richard, D. Scherman and Y. Liu, *J. Mater. Chem. B*, 2019, **7**, 3796–3803.

43 V. Günther, U. Lindert and W. Schaffner, *Biochim. Biophys. Acta, Mol. Cell Res.*, 2012, **1823**, 1416–1425.

44 H. Kusuhara and Y. Sugiyama, *NeuroRx*, 2005, **2**, 73–85.

45 M. Schweigel-Röntgen, in Current Topics in Membranes, ed. M. O. Bevensee, Academic Press, 2014, vol. 73, pp. 321–355

46 M. W. Pfaffl, A. Tichopad, C. Prgomet and T. P. Neuvians, *Biotechnol. Lett.*, 2004, **26**, 509–515.

47 K. J. Livak and T. D. Schmittgen, *Methods*, 2001, **25**, 402–408.

48 R. Fischer and O. Maier, Interrelation of Oxidative Stress and Inflammation in Neurodegenerative Disease, https://www.hindawi.com/journals/omcl/2015/610813/ , (accessed April 9, 2020)

49 T. Ishida, K. Masuda, T. Ichikawa, M. Ichihara, K. Irimura and H. Kiwada, *Int. J. Pharm.*, 2003, **255**, 167–174.

50 X. Wang, T. Ishida and H. Kiwada, *J. Controlled Release*, 2007, **119**, 236–244.

51 C. Richard and B. Viana, Persistent X-ray-activated phosphors: mechanisms and applications, *Light: Science & Applications*, 2022, **11**, 123, DOI: 10.1038/s41377-022-00808-6.

Footnotes

[†] Electronic supplementary information (ESI) available. See DOI: https://doi.org/10.1039/d2nr03546d

Queries and Answers

Q1

Query: Funder details have been incorporated in the funder table using information provided in the article text. Please check that the funder information in the table is correct and indicate any changes, if required. If changes are required, please ensure that you also amend the Acknowledgements text as appropriate.

Answer: ok

Q2

Query: For your information: You can cite this article before you receive notification of the page numbers by using the following format: (authors), Nanoscale, (year), DOI: 10.1039/d2nr03546d.

Answer: ok

Q3

Query: Have all of the author names been spelled and formatted correctly? Names will be indexed and cited as shown on the proof, so these must be correct. No late corrections can be made.

Answer: only one author is not correctly written: Thomas Lecuyer should be replaced by Thomas Lécuyer

Q4

Query: Do you wish to add an e-mail address for the corresponding author? If so, please provide the relevant information.

Answer: Florence Gazeau: florence.gazeau@univ-paris-diderot.fr

Cyrille Richard: cyrille.richard@u-paris.fr

Q5

Query: Please check that the inserted Graphical Abstract text is suitable. If you provide replacement text, please ensure that it is no longer than 250 characters (including spaces).

Answer: remove the inserted graphical abstract text and use this one:

A one-year fellow up of ZGO nanoparticles in vivo: protocol and characterizations

Q6

Query: In the sentence beginning “In contrast to molecular …”, a word or phrase appears to be missing before “shape”. Please check this carefully and indicate any changes required.

Answer: it is OK like this

Q7

Query: The sentence beginning “Blood count measurements…” has been altered for clarity. Please check that the meaning is correct.

Answer: ok

Q8

Query: In the sentence beginning “.25 µL of each diluted …” should “assays” and “assay” be changed to “assay reagent”?

Answer: no it is ok like this

Q9

Query: In the sentences beginning “Each 6 µL Master …” and “The samples and assays” should “assay(s)” be changed to “assay reagent(s)”?

Answer: no it is ok like this

Q10

Query: A citation to ref. 47 has been inserted in the sentence beginning “Data analysis was...”, please check that the placement of this citation is suitable. If the inserted citation is not suitable, please indicate whether this should be changed to a citation to a different reference.

Answer: yes

Q11

Query: In the sentence beginning “Similarly, to ZGOOH, no …” should “Similarly, to” be changed to “Similar to” or “Similarly, in the case of”?

Answer: Similarly to ZGOOH, no luminescence...

Q12

Query: In the sentence beginning “Overall the presence …” should “barely not degraded” be changed to “barely degraded”?

Answer: barely degraded

Q13

Query: Have all of the funders of your work been fully and accurately acknowledged? If not, please ensure you make appropriate changes to the Acknowledgements text.

Answer: ok

Q14

Query: Ref. 11: Can this reference be updated? If so, please provide the relevant information such as year, volume and page or article numbers as appropriate.

Answer: Adv. Drug Deliv. Rev., 2019, 138, 193-210.

Q15

Query: Ref. 20: Please provide the page (or article) number(s).

Answer: Nanoscale, 2022, 14, 1386-1394.

Q16

Query: Ref. 23: Please provide the initial(s) for the 1st author.

Answer: J. Balasubramanian ...

Q17

Query: Ref. 35: Please provide the year of publication and the page (or article) number(s).

Answer: *J Enzymol Metab*. 2015, 1(1):101.

Q18

Query: Ref. 36: Please provide the full list of author names (including initials), the year of publication and the page (or article) number(s).

Answer: A. Baranska, A. Shawket, M. Jouve, M. Baratin, C. Malosse, O. Voluzan, T.-P. Vu Manh,F. Fiore, M. Bajénoff, P. Benaroch, M. Dalod, M. Malissen, S. Henri, B. Malissen, J. Exp. Med. 2018, 215, 1115–1133